4. Wada T, Furuichi K, Sakai N, Iwata Y, Yoshimoto K, Shimizu M, Takeda SI, Takasawa K, Yoshimura M, Kida H, Kobayashi KI, Mukaida N, Naito T, Matsushima K, Yokoyama H. Up-regulation of MCP-1 in tubulointerstitial lesions of human diabetic nephropathy. Kidney Int. 2000;58:1492–9.
5. Cooper ME. Pathogenesis, prevention, and treatment of diabetic nephropathy. Lancet. 1998;352:213–9.
6. Navarro-gonzalez JF, Mora-Fernandez C, Muros de Fuentes M, Garcia-Perez J. Inflammatory molecules and pathways in the pathogenesis of diabetic nephropathy. Nat Rev Nephrol. 2011;7:327–40.
7. Sakai N, Wada T, Furuichi K, Iwata Y, Yoshimoto K, Kitagawa K, Kokubo S, Kobayashi M, Hara A, Yamahana J, Okumura T, Takasawa K, Takeda S, Yoshimura M, Kida H, Yokoyama H. Involvement of extracellular signal-regulated kinase and p38 in human diabetic nephropathy. Am J Kidney Dis. 2005;45:54–65.
8. Wada T, Yokoyama H, Furuichi K, Kobayashi KI, Harada K, Naruto M, Su SB, Akiyama H, Mukaida N, Matsushima K. Intervention of crescentic glomerulonephritis by antibodies to monocyte chemotactic and activating factor (MCAF/MCP-1). FASEB J. 1996;10:1418–25.
9. Wada T, Matsushima K, Kaneko S. The role of chemokines in glomerulonephritis. Front Biosci. 2008;13:3966–74.
10. Bucala R, Spiegel LA, Chesney J, Hogan M, Cerami A. Circulating fibrocytes define a new leukocyte subpopulation that mediates tissue repair. Mol Med. 1994;1:71–81.
11. Wada T, Sakai N, Sakai Y, Matsushima K, Kaneko S, Furuichi K. Involvement of bone-marrow-derived cells in kidney fibrosis. Clin Exp Nephrol. 2011;15:8–13.
12. Moore BB, Kolodsick JE, Thannickal VJ, Cooke K, Moore TA, Hogaboam C, Wilke CA, Toews GB. CCR2-mediated recruitment of fibrocytes to the alveolar space after fibrotic injury. Am J Pathol. 2005;166:675–84.
13. Wada T, Sakai N, Matsushima K, Kaneko S. Fibrocytes: a new insight into kidney fibrosis. Kidney Int. 2007;72:269–73.
14. Sakai N, Wada T, Yokoyama H, Lipp M, Ueha S, Matsushima K, Kaneko S. Secondary lymphoid tissues chemokine (SLC/CCL21)/CCR7 signaling regulates fibrocytes in renal fibrosis. Proc Natl Acad Sci USA. 2006;103:14098–103.
15. Sakai N, Furuichi K, Shinozaki Y, Yamauchi H, Toyama T, Kitajima S, Okumura T, Kokubo S, Kobayashi M, Takasawa K, Takeda S, Yoshimura M, Kaneko S, Wada T. Fibrocytes are involved in the pathogenesis of human chronic kidney disease. Hum Pathol. 2010;41:672–8.
16. Pilling D, Fan T, Huang D, Kaul B, Gomer RH. Identification of markers that distinguish monocyte-derived fibrocytes from monocytes, macrophages, and fibroblasts. PLoS One. 2009;4:e7475.
17. Reilkoff RA, Bucala R, Herzog EL. Fibrocytes: emerging effector cells in chronic inflammation. Nat Rev Immunol. 2011;11:427–35.
18. Phillips RJ, Burdick MD, Hong K, Lutz MA, Murray LA, Xue YY, Belperio JA, Keane MP, Strieter RM. Circulating fibrocytes traffic to the lungs in response to CXCL12 and mediates fibrosis. J Clin Invest. 2004;114:438–46.
19. Sakai N, Wada T, Matsushima K, Bucala R, Iwai M, Horiuchi M, Kaneko S. The renin-angiotensin system contributes to renal fibrosis through regulation of fibrocytes. J Hypertens. 2008;26:780–90.
20. Lachaal M, Rampal AL, Lee W, Shi Y, Jung CY. GLUT1 transmembrane glucose pathway. Affinity labeling with a transportable D-glucose diazirine. J Biol Chem. 1996;271:5225–30.
21. Ito A, Suganami T, Yamauchi A, Degawa-Yamauchi M, Tanaka M, Kouyama R, Kobayashi Y, Nitta N, Yasuda K, Hirata Y, Kuziel WA, Takeya M, Kanegasaki S, Kamei Y, Ogawa Y. Role of CC chemokine receptor 2 in bone marrow cells in the recruitment of macrophages into obese adipose tissue. J Biol Chem. 2008;283:35715–23.
22. Sakai N, Wada T, Furuichi K, Shimizu K, Kokubo S, Hara A, Yamahana J, Okumura T, Matsushima K, Yokoyama H, Kaneko S. MCP-1/CCR2-dependent loop for fibrogenesis in human peripheral CD14-positive monocytes. J Leukoc Biol. 2006;79:555–63.
23. Kitagawa K, Wada T, Furuichi K, Hashimoto H, Ishiwata Y, Asano M, Takeya M, Kuziel WA, Matsushima K, Mukaida N, Yokoyama H. Blockade of CCR2 ameliorates progressive fibrosis in kidney. Am J Pathol. 2004;165:237–46.
24. Schröppel B, Fischereder M, Wiese P, Segerer S, Huber S, Kretzler M, Heiss P, Sitter T, Schlöndorff D. Expression of glucose transporters in human peritoneal mesothelial cells. Kidney Int. 1998;53:1278–87.
25. Strieter RM, Keeley EC, Hughes MA, Burdick MD, Mehrad B. The role of circulating mesenchymal progenitor cells (fibrocytes) in the pathogenesis of pulmonary fibrosis. J Leukoc Biol. 2009;86:1111–8.
26. Calder PC, Dimitriadis G, Newsholme P. Glucose metabolism in lymphoid and inflammatory cells and tissues. Curr Opin Clin Nutr Metab Care. 2007;10:531–40.
27. Maratou E, Dimitriadis G, Kollias A, Boutati E, Lambadiari V, Mitrou P, Raptis SA. Glucose transporter expression on the plasma membrane of resting and activated white blood cells. Eur J Clin Invest. 2007;37:282–90.
28. Takaishi H, Taniguchi T, Takahashi A, Ishikawa Y, Yokoyama M. High glucose accelerates MCP-1 production via p38 MAPK in vascular endothelial cells. Biochem Biophys Res Commun. 2003;305:122–8.
29. Shanmugam N, Reddy MA, Guha M, Natarajan R. High glucose-induced expression of proinflammatory cytokine and chemokine genes in monocytic cells. Diabetes. 2003;52:1256–64.
30. Morohoshi M, Fujisawa K, Uchimura I, Numano F. Glucose-dependent interleukin-6 and tumor necrosis factor production by human peripheral blood monocytes in vitro. Diabetes. 1996;45:954–9.
31. Janssen U, Sowa E, Marchand P, Floege J, Phillips AO, Radeke HH. Differential expression of MCP-1 and its receptor CCR2 in glucose primed human mesangial cells. Nephron. 2002;92:797–806.
32. Wong TYH, Phillips AO, Witowski J, Topley N. Glucose-mediated induction of TGF-β1 and MCP-1 in mesothelial cells in vitro is osmolality and polyol pathway dependent. Kidney Int. 2003;62:1404–16.
33. Mine S, Okada Y, Tanikawa T, Kawahara C, Tabata T, Tanaka Y. Increased expression levels of monocyte CCR2 and monocyte chemoattractant protein-1 in patients with diabetes mellitus. Biochem Biophys Res Commun. 2006;344:780–5.
34. Shin CS, Moon BS, Park KS, Kim SY, Park SJ, Chung MH, Lee HK. Serum 8-hydroxy-guanine levels are increased in diabetic patients. Diabetes Care. 2001;24:733–7.
35. Cvetković T, Mitić B, Lazarević G, Vlahović P, Antić S, Stefanović V. Oxidative parameters as possible urine markers in patients with diabetic nephropathy. J Diabetes Complicat. 2009;23:337–42.
36. Pedersen SF, Kapus A, Hoffmann EK. Osmosensory mechanisms in cellular and systemic volume regulation. J Am Soc Nephrol. 2011;22:1587–97.
37. Hong KM, Burdick MD, Phillips RJ, Heber D, Strieter RM. Characterization of human fibrocytes as circulating adipocyte progenitors and the formation of human adipose tissue in SCID mice. FASEB J. 2005;19:2029–31.

38. Tarabra E, Giunti S, Barutta F, Salvidio G, Burt D, Deferrari G, Gambino R, Vergola D, Pinach S, Perin PC, Camussi G, Gruden G. Effect of the monocyte chemoattractant protein-1/CC chemokine receptor 2 system on nephrin expression in streptozotocin-treated mice and human cultured podocytes. Diabetes. 2009;58:2109–18.

39. Bellini A, Mattoli S. The role of the fibrocyte, a bone marrow-derived mesenchymal progenitor, in reactive and reparative fibroses. Lab Invest. 2007;87:858–70.

Am J Physiol Renal Physiol 305: F495–F509, 2013.
First published May 22, 2013; doi:10.1152/ajprenal.00642.2012.

Sestrin-2 and BNIP3 regulate autophagy and mitophagy in renal tubular cells in acute kidney injury

Masayuki Ishihara,[1] Madoka Urushido,[2] Kazu Hamada,[1] Tatsuki Matsumoto,[1] Yoshiko Shimamura,[1] Koji Ogata,[1] Kosuke Inoue,[1] Yoshinori Taniguchi,[1] Taro Horino,[1] Mikiya Fujieda,[3] Shimpei Fujimoto,[1] and Yoshio Terada[1]

[1]*Department of Endocrinology, Metabolism and Nephrology, Kochi Medical School, Kochi University, Nankoku, Japan;*
[2]*Center for Innovative and Translational Medicine, Kochi Medical School, Kochi University, Nankoku, Japan; and*
[3]*Department of Pediatrics, Kochi Medical School, Kochi University, Nankoku, Japan*

Submitted 21 November 2012; accepted in final form 16 May 2013

Ishihara M, Urushido M, Hamada K, Matsumoto T, Shimamura Y, Ogata K, Inoue K, Taniguchi Y, Horino T, Fujieda M, Fujimoto S, Terada Y. Sestrin-2 and BNIP3 regulate autophagy and mitophagy in renal tubular cells in acute kidney injury. *Am J Physiol Renal Physiol* 305: F495–F509, 2013. First published May 22, 2013; doi:10.1152/ajprenal.00642.2012.—Autophagy is a cellular recycling process induced in response to many types of stress. However, little is known of the signaling pathways that regulate autophagy during acute kidney injury (AKI). Bcl-2/adenovirus E1B 19 kDa-interacting protein (BNIP)3 and sestrin-2 are the target proteins of hypoxia-inducible factor (HIF)-1α and p53, respectively. The aim of this study was to investigate the roles of BNIP3 and sestrin-2 in oxidative stress-induced autophagy during AKI. We used rat ischemia-reperfusion injury and cultured renal tubular (NRK-52E) cells as in vivo and in vitro models of AKI, respectively. Renal ischemia-reperfusion injury upregulated the expression of BNIP3 and sestrin-2 in the proximal tubules, as measured by immunohistochemical staining and Western blot analysis. In vitro, NRK-52E cells exposed to hypoxia showed increased expression of BNIP3 mRNA and protein in a HIF-1α-dependent manner. In contrast, sestrin-2 mRNA and protein expression were upregulated in a p53-dependent manner after exposure to oxidative stress (exogenous H_2O_2). NRK-52E cells stably transfected with a fusion protein between green fluorescent protein and light chain 3 were used to investigate autophagy. Overexpression of BNIP3 or sestrin-2 in these cells induced light chain 3 expression and formation of autophagosomes. Interestingly, BNIP3-induced autophagosomes were mainly localized to the mitochondria, suggesting that this protein selectively induces mitophagy. These observations demonstrate that autophagy is induced in renal tubules by at least two independent pathways involving p53-sestrin-2 and HIF-1α-BNIP3, which may be activated by different types of stress to protect the renal tubules during AKI.

Bcl-2/adenovirus E1B 19 kDa-interacting protein-3; acute kidney injury; autophagy; mitophagy; sestrin-2

ISCHEMIA is the leading cause of acute kidney injury (AKI) in the adult population. Prominent morphological features of ischemic AKI include effacement and loss of the proximal tubule brush border, patchy loss of tubular cells, focal areas of proximal tubular dilation, and increased apoptosis (9). The mechanisms that dictate the survival or death of renal cells under oxidative stress must be more completely understood before novel therapeutic strategies for the treatment of ischemic AKI can be explored. Proximal renal tubular cells have high rates of ATP consumption and are very sensitive to hypoxia; thus, mitochondrial damage is one of the most important factors in determining the survival of these cells (1, 43).

Autophagy is one of the cellular processes that protect cells from genotoxic stress, oxidative stress, accumulation of misfolded proteins, and nutrient deprivation. We (20) have previously reported results from a study of autophagy in a mouse model of AKI. Autophagy plays roles in the pathogenesis of many diseases, and, in kidney disease, both beneficial and detrimental effects of autophagy have been reported (19–22). Our understanding of autophagy has expanded greatly in recent years, largely due to the identification of the many genes involved and to the development of improved methods to monitor the process, such as green fluorescent protein (GFP)-light chain 3 (LC3) to visualize autophagosomes in vivo (28). A number of groups (17, 25, 35) have demonstrated a close connection between autophagy and mitochondrial turnover. Removal of mitochondria that contain damaged components is accomplished via autophagy (mitophagy). Mitophagy also serves to eliminate the subset of mitochondria producing the most ROS, and episodic removal of mitochondria will reduce the oxidative burden. However, to the best of our knowledge, there have been no investigations of the mitophagy process in renal tubular cells.

Several novel proteins have been reported to regulate autophagy and mitophagy, including sestrin-2 and Bcl-2/adenovirus E1B 19 kDa-interacting protein (BNIP)3. Sestrin-2 expression is regulated mainly by p53 but also by hypoxia-inducible factor (HIF)-1α. Activation of p53 and HIF-1α has been reported in several models of AKI; however, the involvement of p53 signaling in autophagy in renal cells remains unclear. Although sestrin-2 has been reported to induce autophagy in osteosarcoma cells (26), little is known of its role in AKI. BNIP3 contains a single Bcl-2 homology 3 domain and is localized primarily in the mitochondria (6, 11, 24, 48). Overexpression of BNIP3 has been reported to induce mitophagy by triggering mitochondrial depolarization (13, 17, 42). However, little is known of the function of BNIP3 and mitophagy in renal tubular cells. The aim of this study was to investigate the roles of autophagy and mitophagy in AKI in vivo and in vitro and to examine sestrin-2- and BNIP3-mediated signaling in renal tubular cells. Our data demonstrate that autophagy and mitophagy are induced in renal tubules in AKI by at least two independent pathways, p53-sestrin-2 and HIF-1α-BNIP3 pathways, and further suggest that these two pathways may function to protect renal tubules from different types of stress.

Address for reprint requests and other correspondence: Y. Terada, Dept. of Endocrinology, Metabolism and Nephrology, Kochi Medical School, Kochi Univ., Kohasu, Oko-cho, Nankoku 783-8505, Japan (e-mail: terada@kochi-u.ac.jp).

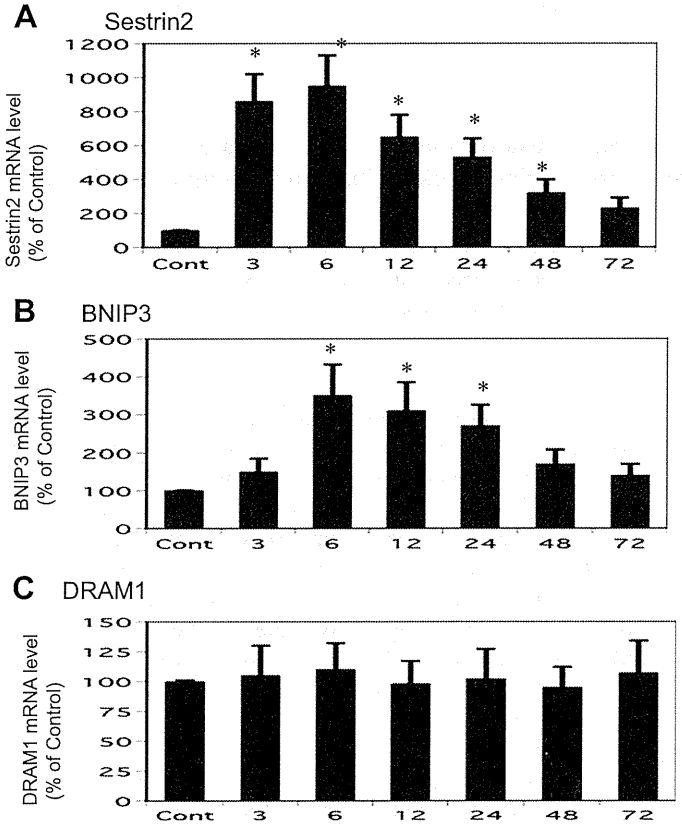

Fig. 1. Real-time quantitative PCR analysis of mRNA expression after ischemic-reperfusion (I/R) acute kidney injury (AKI). Bilateral renal arteries were clamped for 60 min, and kidneys were excised 3, 6, 12, 24, 48, and 72 h after reperfusion. Sham-operated rats euthanized at 0 h served as controls (Cont). Expression of sestrin-2, Bcl-2/adenovirus E1B 19 kDa-interacting protein (BNIP)3, and DNA damage-regulated autophagy modulator (DRAM)1 mRNA was measured by quantitative PCR and normalized to levels of GAPDH mRNA. Data are means ± SE; $n = 5$. *$P < 0.05$ vs. control rats.

MATERIALS AND METHODS

Induction of AKI. Male Sprague-Dawley rats (Saitama Experimental Animal Supply, Saitama, Japan) weighing 150–200 g were anesthetized by an intraperitoneal injection with pentobarbital sodium (30 mg/kg). To induce kidney injury, the left renal artery was occluded with Sugita aneurysm clips (Mizuho Ikakogyo, Tokyo, Japan) for 60 min. The clamps were then removed, and the incisions were closed. Rats were euthanized at 0, 3, 6, 12, 24, 48, and 72 h after surgery ($n = 5$ rats/group). The left kidney was rapidly removed and processed for histological evaluation, protein extraction, and RNA extraction, as previously described (38, 40). Control animals were age- and weight-matched rats that received a sham operation without clamping of the renal arteries and were euthanized at 0 and 12 h ($n = 5$ rats/group). All animal protocols were approved by the Institutional Animal Care and Use Committee of the University of Kochi (no. 20–027), and experiments were conducted in accordance with institutional guidelines.

Cell culture, plasmids, and small interfering RNA. NRK-52E cells (renal tubular cells from an adult rat), originally purchased from American Type Culture Collection (Manassas, VA), were grown in DMEM (GIBCO) supplemented with 50 IU/ml penicillin and 10% heat-inactivated FCS (GIBCO) (38). Cells were cultured at 37°C in a 20% O_2-5% CO_2 atmosphere (referred to as normoxic conditions). For hypoxia experiments, NRK-52E cells were placed in a hypoxic chamber (AnaeroPack, Mitsubishi Gas Chemical) under 0% O_2-5% CO_2 atmosphere and were maintained at 37°C for 2, 4, or 6 h. For H_2O_2 experiments, 200 and 400 μM H_2O_2 was added to NRK-52E cells for the indicated times. Expression vectors encoding wild-type human sestrin-2, BNIP3, and HIF-1α were obtained from Addgene (Rockville, MD) and transfected into NRK-52E cells by electroporation, as previously described (38). Small interfering (si)RNAs specific for sestrin-2 and BNIP3 or control scrambled siRNA were purchased from ABI. NRK-52E cells were transfected with siRNAs by lipofection, as previously described. Western blot analyses were performed to confirm the efficiency of sestrin-2 and BNIP3 knockdown. All other chemicals were purchased from Funakoshi (Tokyo, Japan).

Isolation and histological examination of kidney tissue. Rats were anesthetized with pentobarbital at the indicated times after the ischemic event. The kidneys were perfused in situ with sterile PBS, and the left kidney was then rapidly excised, frozen in liquid nitrogen, and homogenized in SDS sample buffer, as previously described (23). For immunohistochemical experiments, kidneys were fixed in formalin overnight, dehydrated, and embedded in paraffin. Thin sections were cut and subjected to periodic acid-Schiff staining as previously described. Immunohistochemical staining was performed using streptavidin-biotin techniques using antibodies specific to sestrin-2 (cs-292558, Santa Cruz Biotechnology), lysosomal-associated membrane protein (LAMP)1 (cs-35684, Santa Cruz Biotechnology), and BNIP3 (cs-292463, Santa Cruz Biotechnology), as previously described (23, 38). The sequences of anti-sestrin-2- and anti-BNIP3-blocking peptides were CGEEWSQDLHSSGRTDLRYS and CGEEWSQDLHSSGRTDLRYS, respectively (Santa Cruz Biotechnology). Histology sections or immunoblot membranes were preincubated with blocking peptides (10 μg/ml) before the addition of the antibodies.

Western blot analysis. Protein extracts of total renal tissue or NRK-52E cells (50 μg samples) were prepared and denatured by heating at 100°C for 5 min in SDS sample buffer as previously described (41). Proteins were separated on 7.5% or 10–20% polyacrylamide gels and transferred to nitrocellulose membranes. Membranes were blocked for 1 h with 5% (wt/vol) fat-free milk in PBS and probed with the appropriate primary antibodies [anti-LC3 (MBL,

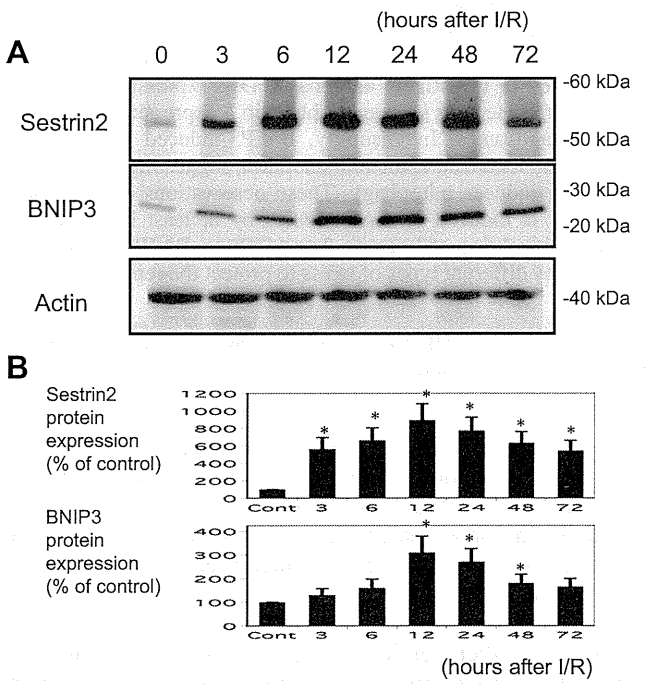

Fig. 2. Western blot analyses of protein expression after I/R AKI. *A*: aliquots of 50 μg protein from renal tissue extracts were separated by SDS-PAGE and transferred to membranes. Sestrin-2 and BNIP3 were detected by Western blot analysis. Actin served as a loading control. *B*: quantitative densitometry was performed for sestrin-2 and BNIP3 blots. Data are means ± SE; $n = 6$. *$P <$ 0.05 vs. control (0 h) by ANOVA.

Nagoya, Japan) or anti-sestrin-2, anti-BNIP3, anti-LAMP1, and anti-actin (H-300, cs-292558, sc-292463, sc-285412, and sc-10731, Santa Cruz Biotechnology)]. Primary antibodies were detected with horseradish peroxidase-conjugated rabbit anti-goat IgG or horseradish peroxidase-conjugated donkey anti-rabbit IgG and visualized using an Amersham ECL system (Amersham, Arlington Heights, IL).

Real-time quantitative PCR. RT-PCR analysis of RNA extracted from kidneys was carried out as previously described (39). In brief, total RNA was isolated from renal tissues using TRI-REAGENT (Life Technologies, Gaithersburg, MD). Samples of total RNA (1 μg) were reverse transcribed, and real-time quantitative PCR was performed to quantify changes in *Sestrin2*, *Bnip3*, and DNA damage-regulated autophagy modulator 1 (*Dram1*) gene expression using the ABI LightCycler real-time PCR system (ABI, Los Angeles CA). RT-PCR of GAPDH served as a positive control. A three-step PCR was performed for 35 cycles. Samples were denatured at 94°C for 30 s, annealed at 58°C for 30 s, and extended at 72°C for 30 s. The primers used were obtained from ABI.

Transient transfection and luciferase assay. The sestrin-2 promoter (−2.5 kb) luciferase plasmid and BNIP3 promoter (−3.7 kb) luciferase plasmid were obtained from Addgene. NRK-52E cells were transfected with plasmid DNA (10 μg) by electroporation, as previously described (34). Luciferase activity was measured 48 h after transfection. Normalization was achieved by cotransfecting cells with a β-galactosidase reporter construct. We established NRK-52E cells stably transfected with an LC3-GFP fusion protein as a marker of autophagy. In these cells, autophagy is indicated by the formation of GFP-positive autophagosomes. For some experiments, NRK-52E cells were cotransfected with a mitochondrial-targeted red fluorescent protein (mitoDsRed, Clontech).

Scanning laser confocal immunofluorescence microscopy and electron microscopy. For confocal microscopy, NRK-52E cells were fixed with 2% paraformaldehyde in PBS for 1 h and processed for imaging as previously described (38). For electron microscopy, cells were fixed in PBS containing 2% paraformaldehyde and 0.1% glutaraldehyde for 2 h. Samples were embedded in Epo-Araldite resin

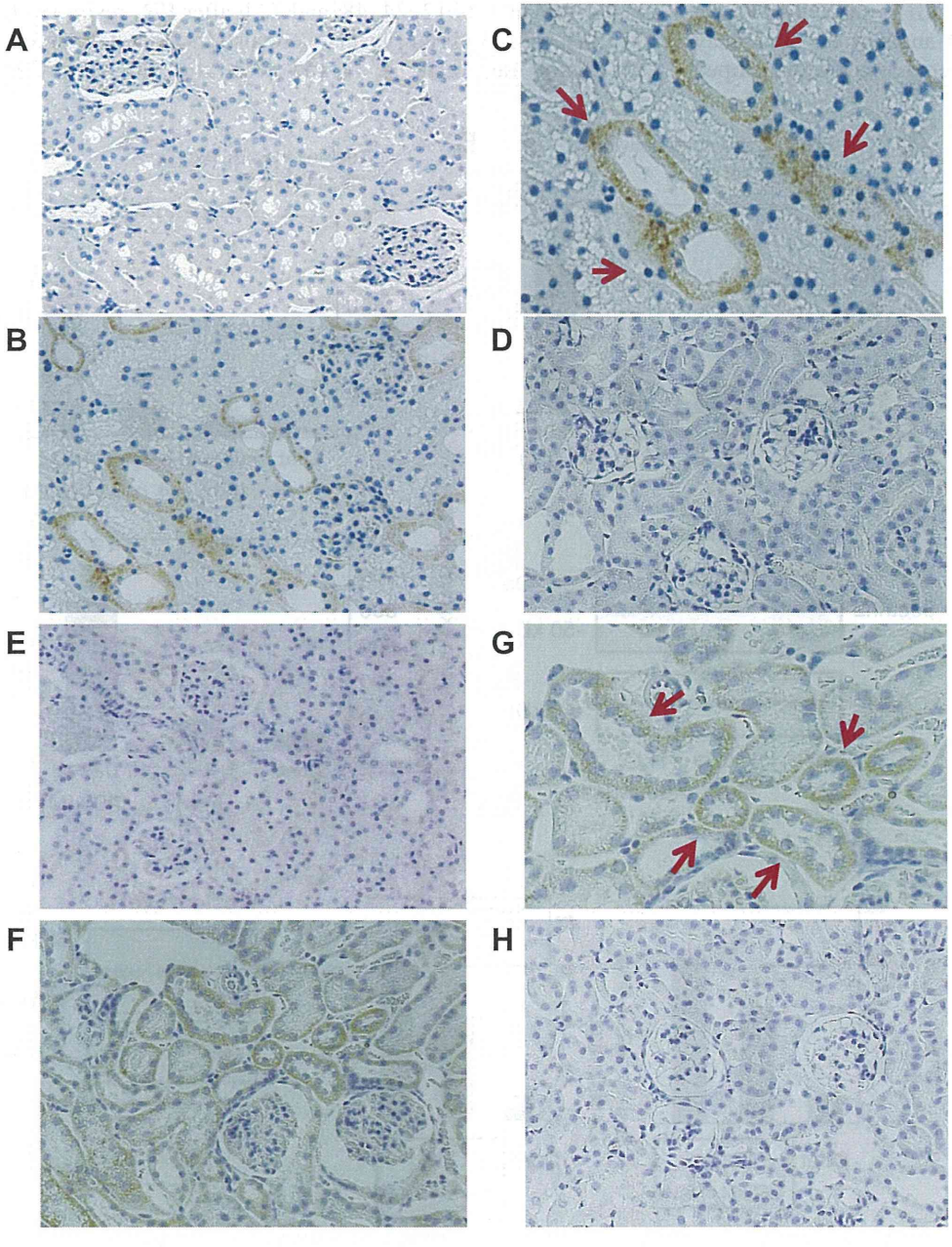

Fig. 3. Immunohistochemical analysis of sestrin-2 and BNIP3 expression after I/R AKI. *A* and *B*: immunohistochemical analysis of sestrin-2 expression in the renal cortex of a control kidney (*A*) or a kidney at 12 h after I/R injury (*B*). Magnification: ×100. *C*: high-power view of the renal cortex stained with anti-sestrin-2 antibody. Magnification: ×600. The arrows indicate sestrin-2-positive cells. *D*: immunohistochemical analysis of sestrin-2 expression in the renal cortex 12 h after I/R injury. Staining was performed in the presence of an anti-sestrin-2-blocking peptide. Magnification: ×100. *E* and *F*: immunohistochemical analysis of BNIP3 expression in the renal cortex of a control kidney (*E*) or a kidney at 12 h after I/R injury (*F*). Magnification: ×100. *G*: high-power view of the renal cortex stained with an anti-BNIP3 antibody. Magnification: ×600. The arrows indicate BNIP3-positive cells. *H*: immunohistochemical analysis of BNIP3 expression in the renal cortex at 12 h after I/R injury. Staining was performed in the presence of an anti-BNIP3-blocking peptide.

(Canemco), and ultrathin sections were cut under a Reichert ultramicroscope; these sections were counterstained with 0.3% lead citrate and examined under a Philips EM420 electron microscope.

Caspase-3 assay and TUNEL assay. A Caspase-3 Fluorometric Protease Assay Kit (MBL) was used for the measurement of caspase-3 activity, as previously described (39). In brief, cell lysates were incubated with reaction buffer and 50 mM caspase-3 substrate for 2 h at 37°C, and the enzymatic activity was measured colorimetrically. The Apoptosis TUNEL Kit II (MBL) was used for the staining for TUNEL-positive cells, as previously described (39).

Statistics. Results are presented as means ± SE. Differences between the groups were tested by two-way ANOVA followed by Scheffé's test for multiple comparisons. Two groups were compared using unpaired *t*-tests. *P* values of <0.05 were considered statistically significant.

RESULTS

Sestrin-2 and BNIP3 gene expression after ischemic AKI in vivo. To examine the effects of ischemia-reperfusion (I/R) injury on the expression of sestrin-2, BNIP3, and DRAM1, we conducted real-time quantitative PCR analysis on rat kidney tissues. To induce I/R injury, the left renal artery was clamped for 60 min, and the kidney was excised from animals euthanized at 3, 6, 12, 24, 48, and 72 h after reperfusion. Kidneys from sham-operated rats were used as controls (0 h). Quantitative PCR analysis revealed dramatic changes in sestrin-2 and BNIP3 mRNA levels after I/R, but there was no effect on DRAM1 gene expression under our experimental conditions. Sestrin-2 mRNA levels were significantly increased compared with those in the controls between 3 and 48 h postischemia, and BNIP3 mRNA levels were dramatically elevated between 6 and 24 h after I/R injury (Fig. 1).

Sestrin-2 and BNIP3 protein expression after ischemic AKI in vivo. Western blot analyses were performed on kidney extracts to determine if I/R induced changes in the expression of sestrin-2 and BNIP3 protein. Consistent with the quantitative PCR results, sestrin-2 protein expression was markedly increased between 3 and 72 h after I/R compared with control rats (Fig. 2*A*). Quantitative densitometry of the blots revealed that sestrin-2 levels were increased 5.6-, 6.6-, 8.9-, 7.7-, 6.3-, and 5.4-fold at 3, 6, 12, 24, 48, and 72 h after I/R, respectively (Fig. 2*B*). BNIP3 protein levels were also increased compared with control rats between 12 and 48 h after I/R (Fig. 2*A*).

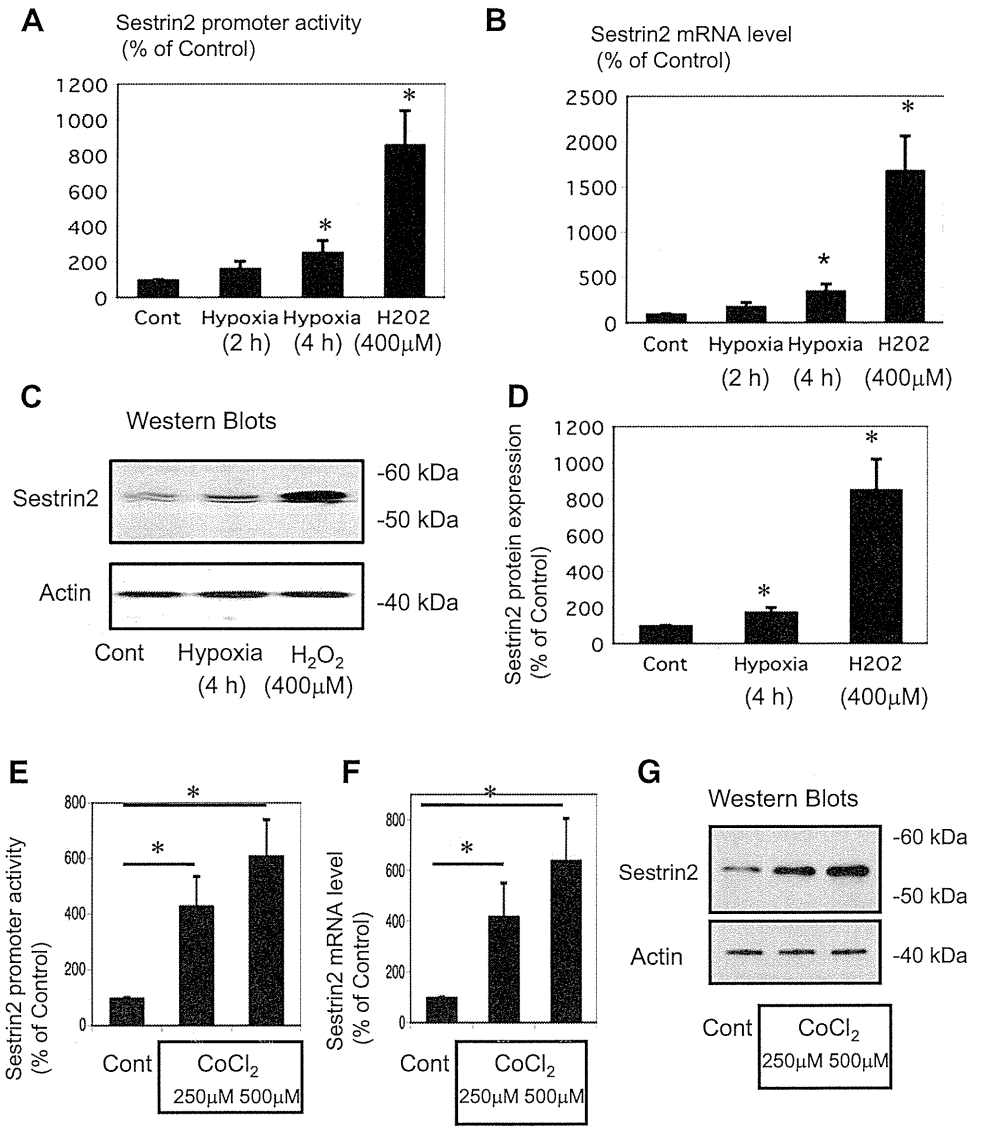

Fig. 4. Analysis of sestrin-2 promoter activity, mRNA levels, and protein expression in NRK-52E cells subjected to oxidative stress. NRK-52E cells were exposed to hypoxia (2 or 4 h) or H_2O_2 (400 μM). *A*: sestrin-2 promoter activity was measured by luciferase assays. *B*: sestrin-2 mRNA levels were measured by PCR. *C*: sestrin-2 protein expression was measured by Western blot analysis. *D*: densitometric analysis of sestrin-2 protein expression after exposure to hypoxia (4 h) and H_2O_2 (400 μM). Cells were incubated with $CoCl_2$ (250 or 500 μM) for 6 h. *E*: sestrin-2 promoter activity was measured by luciferase assays. *F*: sestrin-2 mRNA levels were measured by RT-PCR. *G*: sestrin-2 protein expression was measured by Western blot analysis. Data are means ± SE; $n = 5$. *$P < 0.05$ vs. control-treated cells.

BNIP3 was only weakly expressed in control and sham-operated kidneys. BNIP3 levels were increased by 3.1-, 2.7-, and 1.8-fold at 12, 24, and 48 h after I/R, respectively, compared with control animals (Fig. 2*B*).

Immunohistochemical examination of sestrin-2 and BNIP3 expression in ischemic AKI. Next, we performed immunohistological experiments of sestrin-2 and BNIP3 expression in I/R AKI (Fig. 3). Under low-power microscopy, sestrin-2 and BNIP3 expression were observed in cortical renal tubules at 12 h after I/R (Fig. 3, *B* and *F*), and high-power views indicated that both proteins were localized mainly to the cytoplasm (Fig. 3, *C* and *G*). In contrast, only low levels of sestrin-2 and BNIP3 were detected in the cortical renal tubules of control rats (Fig. 3, *A* and *E*). To confirm the specificity of the anti-sestrin-2 and anti-BNIP3 antibodies, immunostaining was also performed in the presence of antigen-specific blocking peptides (Santa Cruz Biotechnology), which resulted in diminished cytoplasmic staining in cortical cells of I/R-injured kidneys (Fig. 3, *D* and *H*). These results demonstrate that sestrin-2 and BNIP3 were expressed mainly in the proximal tubules of the renal cortex 12 h after I/R.

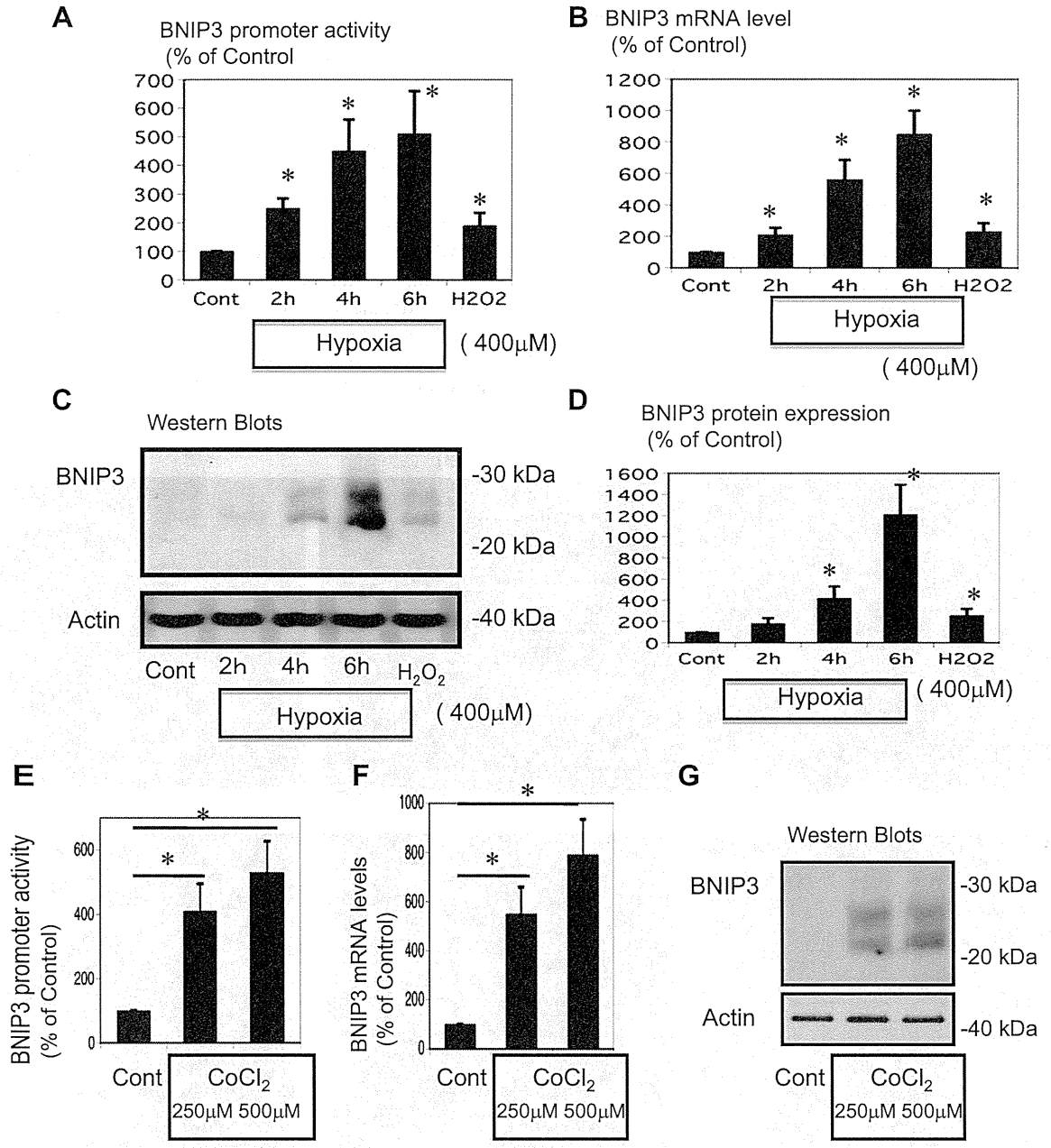

Fig. 5. Analysis of BNIP3 promoter activity, mRNA levels, and protein expression in NRK-52E cells exposed to hypoxia or H_2O_2. *A*: cells were exposed to hypoxia (2, 4, or 6 h) and H_2O_2 (400 μM), and BNIP3 promoter activity was assessed. *B* and *C*: cells were exposed to hypoxia (2, 4, or 6 h) or H_2O_2 (400 μM), and BNIP3 mRNA was measured by PCR (*B*) and BNIP3 protein expression was measured by Western blot analysis (*C*). *D*: densitometric analysis of BNIP3 protein expression after exposure to hypoxia (2, 4, or 6 h) and H_2O_2 (400 μM). Cells were incubated with $CoCl_2$ (250 and 500 μM) for 6 h. *E*: BNIP3 promoter activity was measured by luciferase assays. *F*: BNIP3 mRNA levels were measured by PCR. *G*: BNIP3 protein expression was measured by Western blot analysis. Data are means ± SE; $n = 5$. *$P < 0.05$ vs. control-treated cells.

Increased sestrin-2 promoter activity and mRNA and protein expression in H_2O_2-treated NRK-52E cells in vitro. To determine if sestrin-2 expression is induced by oxidative stress in renal cells, we examined sestrin-2 promoter activity, mRNA levels, and protein expression in cultured NRK-52E cells exposed to hypoxia and H_2O_2. We found that sestrin-2 promoter activity was significantly increased by hypoxia and H_2O_2 compared with control normoxia cells (Fig. 4*A*). Similarly, sestrin-2 mRNA levels were significantly increased under the same conditions. Compared with control cells, H_2O_2 treatment increased sestrin-2 mRNA expression by 17.5-fold (Fig. 4*B*). Consistent with the effects on mRNA expression, hypoxia induced a small but significant increase in sestrin-2 (Fig. 4, *C* and *D*). However, H_2O_2 treatment caused a marked increase in sestrin-2 expression (8.9-fold; Fig. 4, *C* and *D*). To examine the signaling pathway of sestrin-2 induction by hypoxia and oxidative stress, we used $CoCl_2$, a well-known activator of HIF-1α. As shown in Fig. 4, *E–G*, $CoCl_2$ dose dependently stimulated sestrin-2 promoter activity up to 6.1-fold, increased mRNA expression up to 6.2-fold, and increased protein expression up to 5.3-fold in NRK-52E cells.

Increased BNIP3 promoter activity and mRNA and protein expression in NRK-52E cells exposed to hypoxia or H_2O_2. BNIP3 promoter activity and mRNA expression in NRK-52E cells were increased significantly by both hypoxia and H_2O_2, with hypoxia having a greater effect (Fig. 5, *A* and *B*). Compared with control cells, hypoxic treatment increased BNIP3 mRNA expression by 8.3-fold (Fig. 5*B*). BNIP3 protein levels were increased by cell exposure to hypoxia and H_2O_2 (Fig. 5, *C* and *D*). Consistent with the effects on mRNA expression, H_2O_2 induced a small but significant increase in BNIP3 (Fig. 5, *C* and *D*). However, hypoxia caused a marked increase in BNIP3 expression (12.6-fold; Fig. 5, *C* and *D*). To examine the signaling pathway of BNIP3 induction by hypoxia and oxidative stress, we used $CoCl_2$, a well-known activator of HIF-1α. As shown in Fig. 5, *E–G*, $CoCl_2$ dose dependently stimulated BNIP3 promoter activity up to 5.3-fold, increased mRNA expression up to 7.9-fold, and increased protein expression up to 9.7-fold in NRK-52E cells. We also observed by confocal microscopy that the hypoxic conditions increased BNIP3 expression in the cytoplasm of NRK-52E cells (Fig. 6).

Time courses of LC3-II and LAMP1 accumulation in oxidative stress in NRK-52E cells. To monitor autophagic flux in renal tubular cells during oxidative stress, we examined the time course of LC3-II and LAMP1 accumulation in cells incubated with H_2O_2. We used LC3-II and LAMP1 as markers of autophagy induction and autophagic flux. As shown in Fig. 7*A*, Western blot analysis showed that LC3-II expression was increased between 4 and 8 h after oxidative stress and that LAMP1 increased between 8 and 12 h. In the experiment examining oxidative stress by confocal microscopy, only LC3-II punctae were detected at 4 h, colocalized LC3-II and LAMP1 punctae were seen at 8 h, and only LAMP1 punctae were detected at 12 h (Fig. 7*B*). LAMP1 expression therefore followed LC3-II expression.

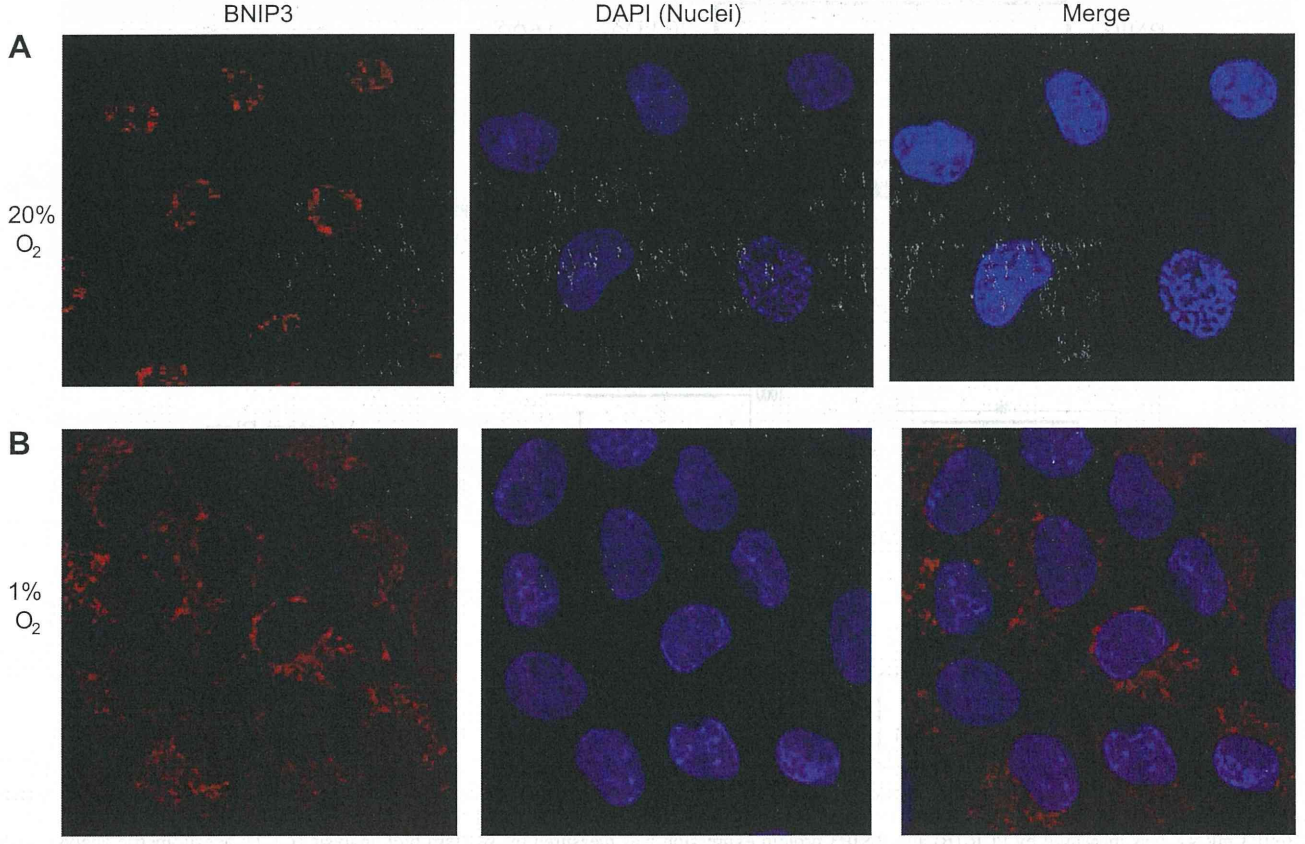

Fig. 6. Analysis of BNIP3 protein expression in NRK-52E cells exposed to hypoxia by confocal micrpscopy. NRK-52E cells were incubated under normoxic (*A*) or hypoxic (*B*) conditions and examined by confocal microscopy for BNIP3 expression. Cells were counterstained with 4′,6-diamidino-2-phenylindole (DAPI) to visualize nuclei. Original magnification: ×400.

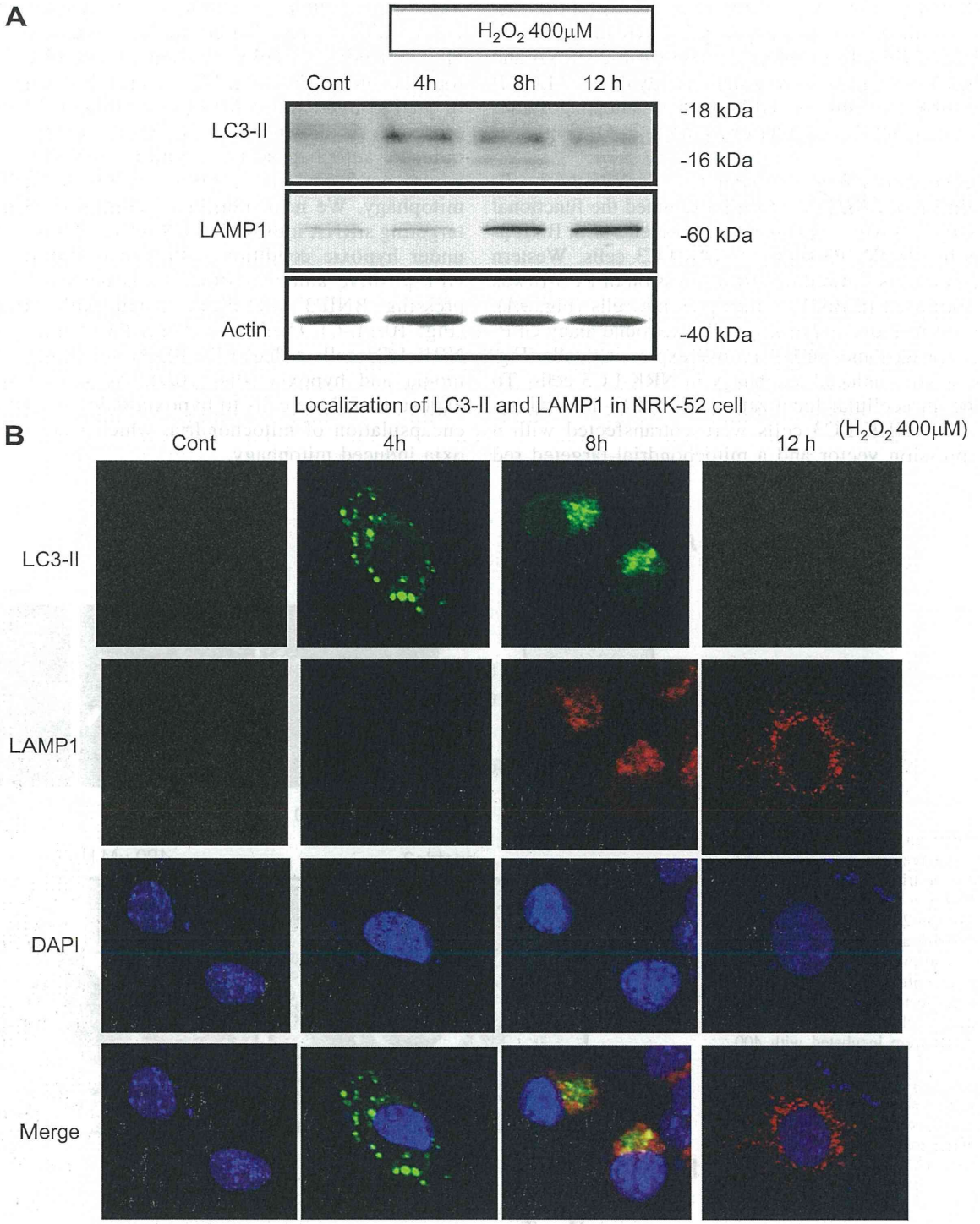

Fig. 7. Time course and intracellular localization of light chain 3 (LC3)-II and lysosomal-associated membrane protein (LAMP)1 in NRK-52E cells. NRK-52E cells were exposed to 400 μM H_2O_2 to induce oxidative stress. *A*: aliquots of 50 μg protein from NRK-52E cell extracts were separated by SDS-PAGE and transferred to membranes. LC3-II and LAMP1 were detected by Western blot analysis. Actin served as a loading control. *B*: confocal microscopy of green fluorescent protein (GFP)-positive autophagosomes (green) and LAMP1 (red) was performed in NRK-LC3-II cells after exposure to 400 μM H_2O_2 for the indicated times.

Modulation of autophagy in NRK-LC3 cells by manipulation of sestrin-2 levels. To examine the functional role of sestrin-2 in autophagy, we transiently transfected NRK-LC3 cells (NRK-52E cells stably expressing GFP-LC3) with control or sestrin-2 expression vectors. Western blot analysis of cell extracts showed that expression of the autophagy marker LC3-II was markedly increased in cells that overexpressed sestrin-2 compared with control cells (Fig. 8*A*). In addition, many GFP-positive autophagosomes were visible in sestrin-2-overexpressing cells by confocal microscopy (Fig. 8*B*). Furthermore, autophagosome formation was observed in electron micrographs of sestrin-2-overexpressing cells and cells incu-

bated with H_2O_2 (Fig. 8*C*). These data clearly show that sestrin-2 expression induced autophagy in NRK-LC3 cells. In contrast, NRK-LC3 cells transfected with sestrin-2 siRNA and then incubated with H_2O_2 showed significantly reduced LC3-II expression and numbers of GFP-positive autophagosomes compared with control cells after exposure to H_2O_2 (Fig. 8, *D* and *E*).

Modulation of autophagy and mitophagy in NRK-LC3 cells by manipulation of BNIP3 levels. We examined the functional role of BNIP3 by performing similar experiments with BNIP3-overexpressing or BNIP3-silenced NRK-LC3 cells. Western blots of cell extracts showed that the expression of LC3-II was markedly increased in BNIP3-overexpressing cells (Fig. 9*A*). Similar to sestrin-2-overexpressing cells, we found many GFP-positive autophagosomes in BNIP3-overexpressing cells (Fig. 9*B*). Thus, BNIP3 induced autophagy in NRK-LC3 cells. To examine the intracellular localization of BNIP3-induced autophagosomes, NRK-LC3 cells were cotransfected with a BNIP3 expression vector and a mitochondrial-targeted red fluorescent protein (mitoDsRed). By confocal microscopy, many GFP and mitoDsRed double-positive foci were visible, indicative of colocalization of mitochondria and autophagosomes (Fig. 9*C*). Moreover, mitophagy was evident in BNIP3-overexpressing cells examined by electron microscopy. As shown in Fig. 9*D*, BNIP3-overexpressing cells induced autophagosomal encapsulation of mitochondria, which confirmed that overexpression of BNIP3 induced mitophagy. We next transfected control siRNA or BNIP3-targeting siRNA into NRK-LC3 cells and incubated the cells under hypoxic conditions. We found that the number of GFP-positive autophagosomes was decreased in cells expressing BNIP3 siRNA compared with control siRNA (Fig. 10, *A–C*). Furthermore, BNIP3-targeting siRNA into NRK-LC3 cells reduced LC3-II protein levels in both normoxia and hypoxia (Fig. 10*D*). As shown in Fig. 10*E*, exposure of these cells to hypoxia induced autophagosomal encapsulation of mitochondria, which confirmed that hypoxia induced mitophagy.

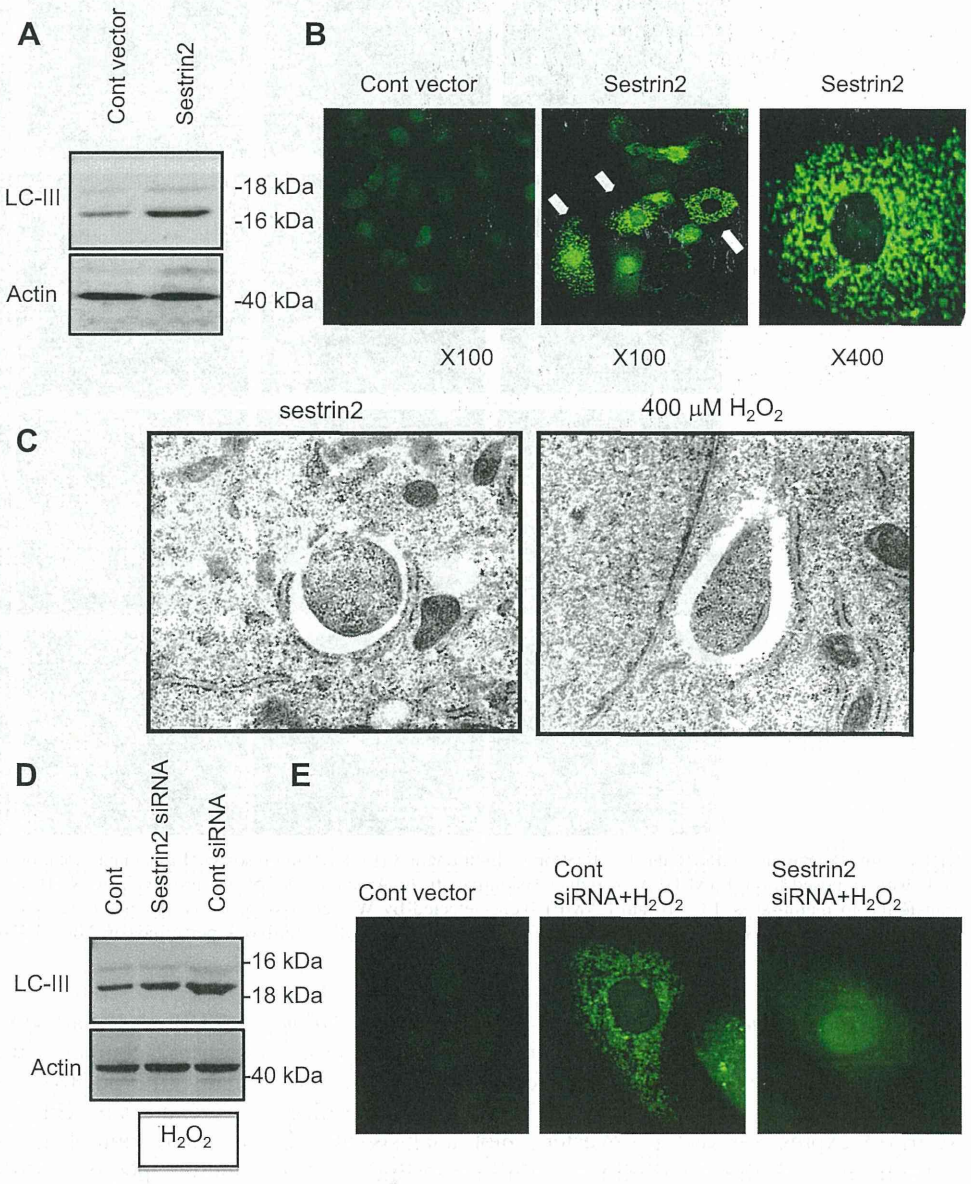

Fig. 8. Autophagy in NRK-LC3 cells is increased by overexpression of sestrin-2 and suppressed by sestrin-2 small interfering (si)RNA. *A*: Western blot analysis of LC3-II in control or sestrin-2-overexpressing NRK-52E cells. *B*: confocal microscopy of GFP-positive autophagosomes in NRK-LC3 cells transfected with control or sestrin-2 expression vectors. *C*: electron microscopy of autophagosomes in cells that overexpressed sestrin-2 (*left*) or were incubated with 400 μM H_2O_2 (*right*). *D*: Western blot analysis of LC3-II in control or sestrin-2 siRNA-transfected NRK-52E cells incubated with 400 μM H_2O_2. *E*: confocal microscopy of GFP-positive autophagosomes in sestrin-2 siRNA-transfected NRK-LC3 cells incubated with 400 μM H_2O_2.